Electronic Supplementary Information for

Energy-efficient hydrogen production coupled with simultaneous electrosynthesis of acetate over mesoporous OsRh film

Ziqiang Wang, Peng Wang, Hugang Zhang, Kai Deng, Hongjie Yu, You Xu, Xiaonian Li, Hongjing Wang and Liang Wang*

State Key Laboratory Breeding Base of Green-Chemical Synthesis Technology, College of Chemical Engineering, Zhejiang University of Technology, Hangzhou 310014, P. R. China.

Corresponding author

*E-mail: wangliang@zjut.edu.cn

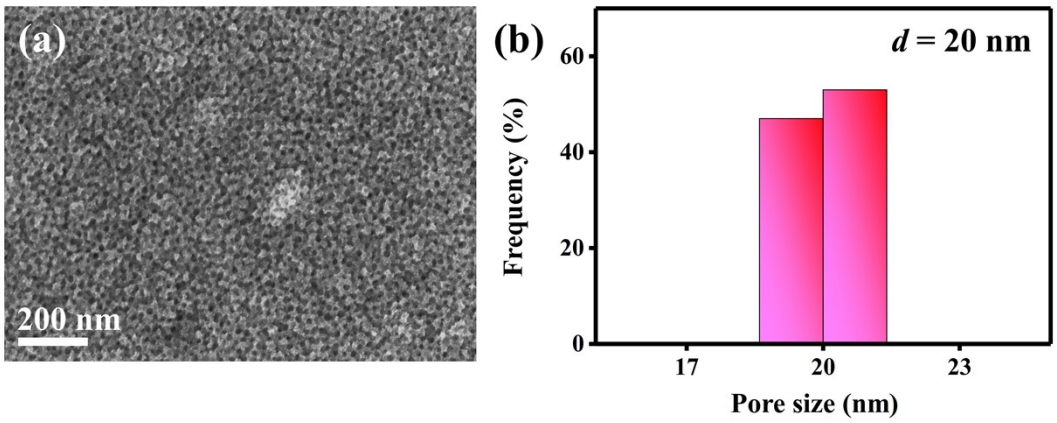

Fig. S1 (a) SEM image and (b) pore size distribution of the mesoporous OsRh/NF.

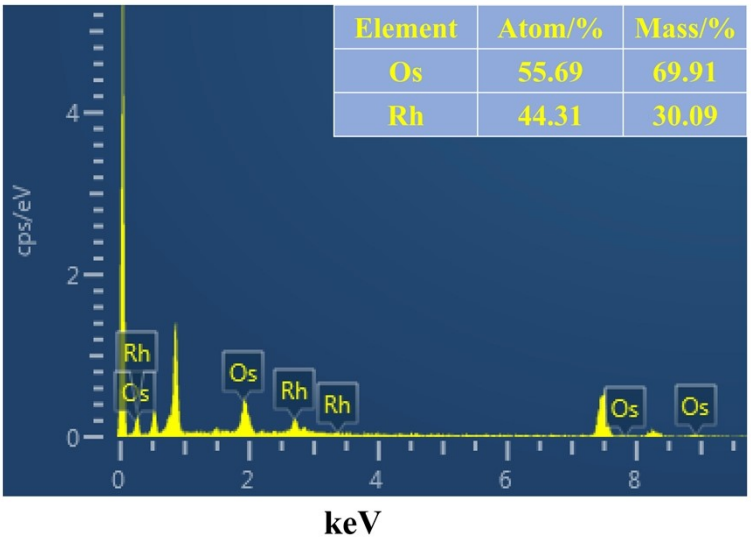

Fig. S2 EDX spectrum of the mOsRh/NF.

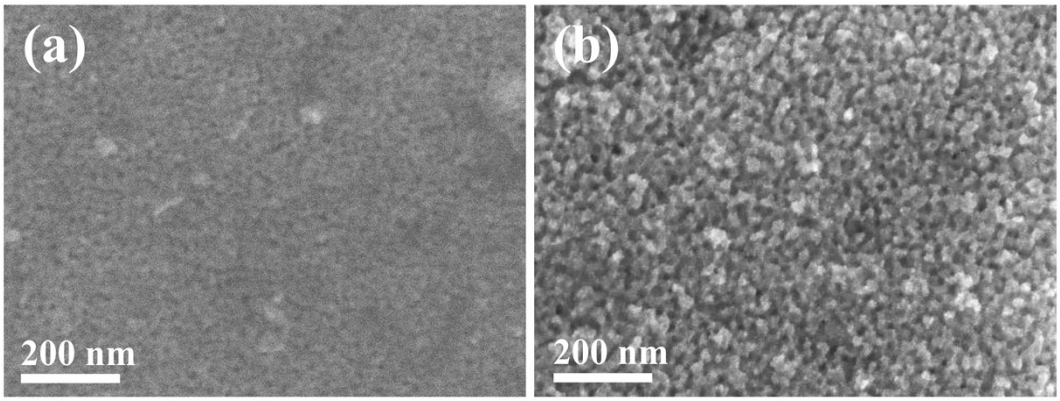

Fig. S3 SEM images of the samples prepared with mono-metallic precursor solutions under typical conditions, (a) K_2OsCl_6 and (b) K_3RhCl_6.

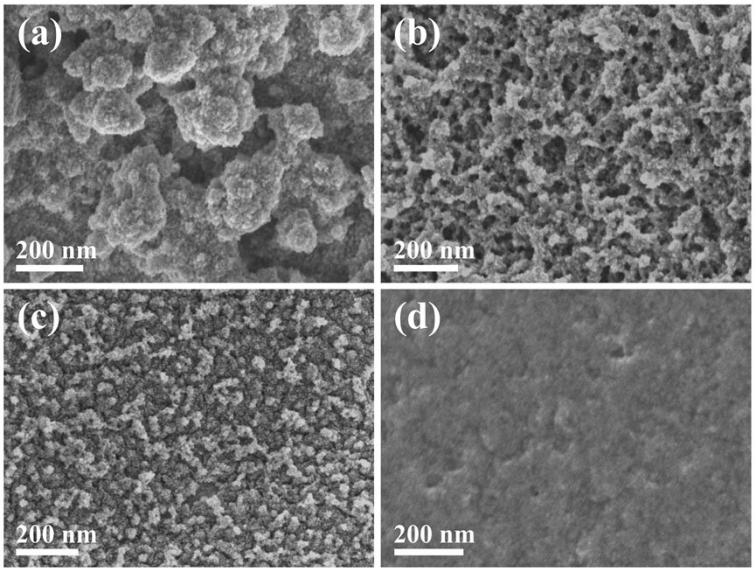

Fig. S4 SEM images of the mOsRh/NF prepared by replacing PEO-*b*-PMMA with (a) PS-*b*-PEO (b) F127 (c) CTAB and (d) no surfactant under the typical condition.

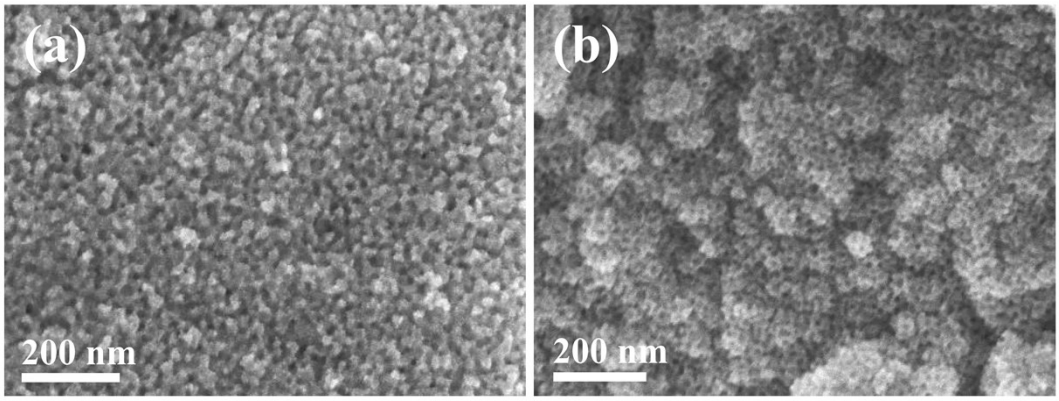

Fig. S5 SEM images of the samples prepared with different ratios of metallic precursor solutions under typical conditions, the amounts of K_2OsCl_6 and K_3RhCl_6 are (a) 2:2 and (b) 1:3.

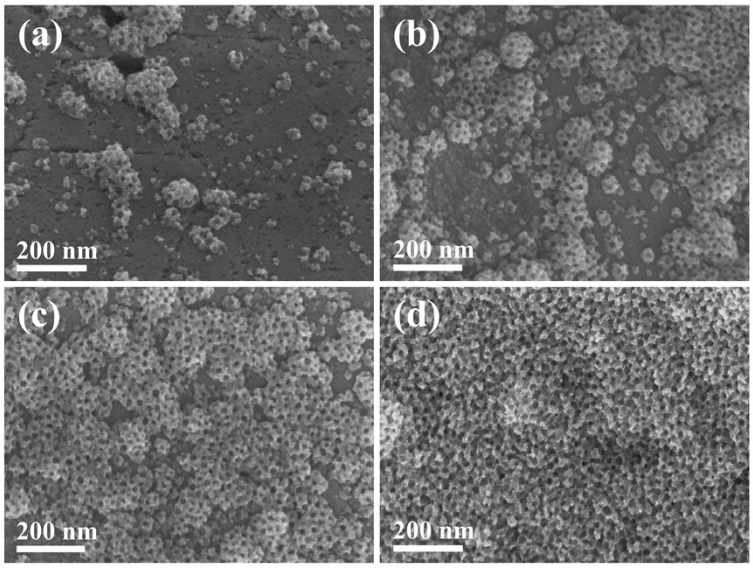

Fig. S6 SEM images of samples prepared under typical conditions for different times: (a) 500, (b) 1000, (c) 2000, and (d) 4000 s.

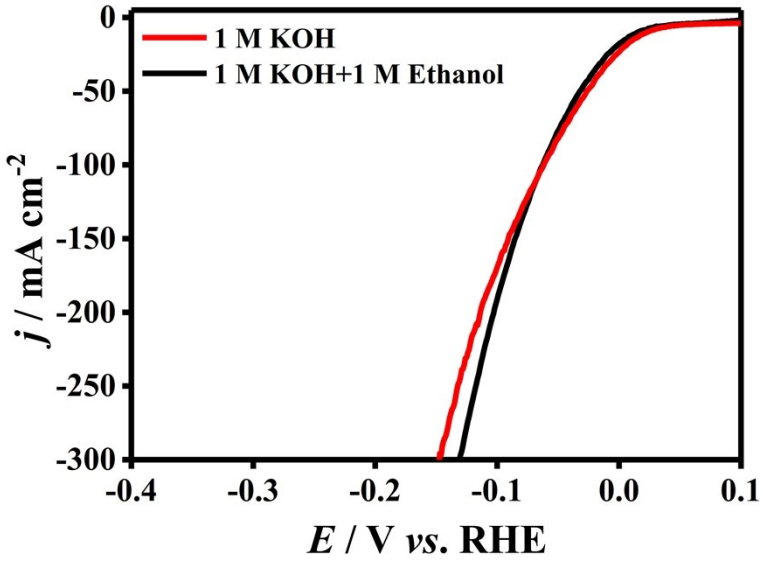

Fig. S7 LSV polarization curves of the mOsRh/NF for HER in 1 M KOH with and without 1 M ethanol.

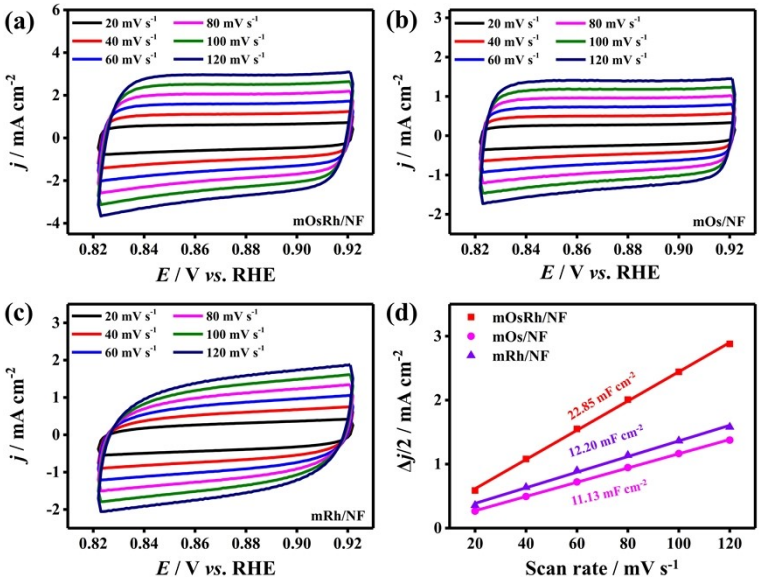

Fig. S8 (a-c) Cyclic voltammograms of different samples at the potential range of 0.82 and 0.92 V. (d) Capacitive current densities at 0.87 V derived from CVs against scan rates for different samples.

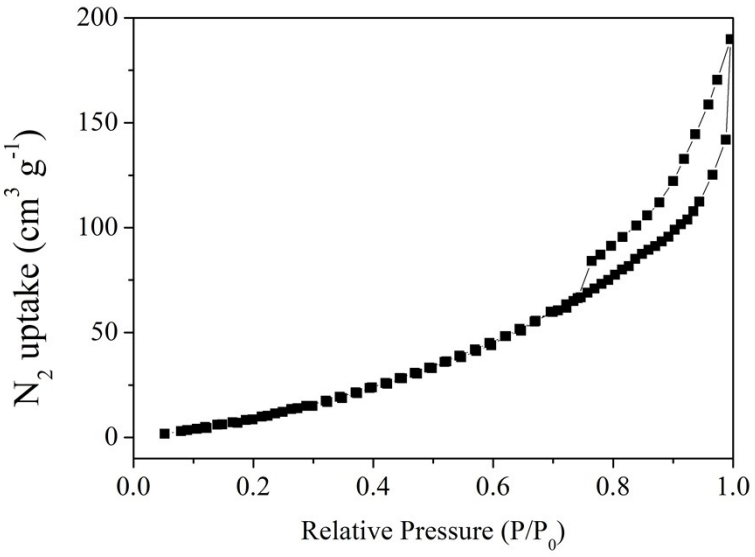

Fig. S9 The nitrogen adsorption-desorption isothermal curve of mesoporous OsRh films scraped NF.

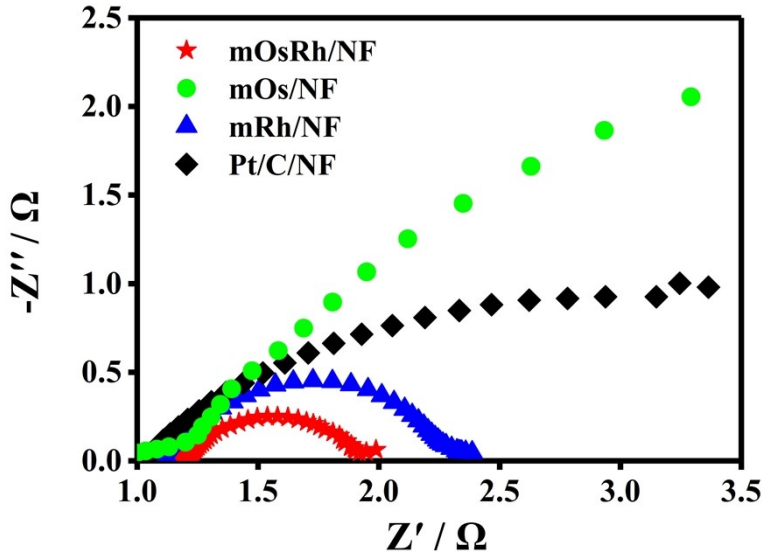

Fig. S10 Nyquist plots for different catalysts obtained in 1 M KOH at overpotential of 20 mV. The frequency ranges from 100 kHz to 0.1 Hz.

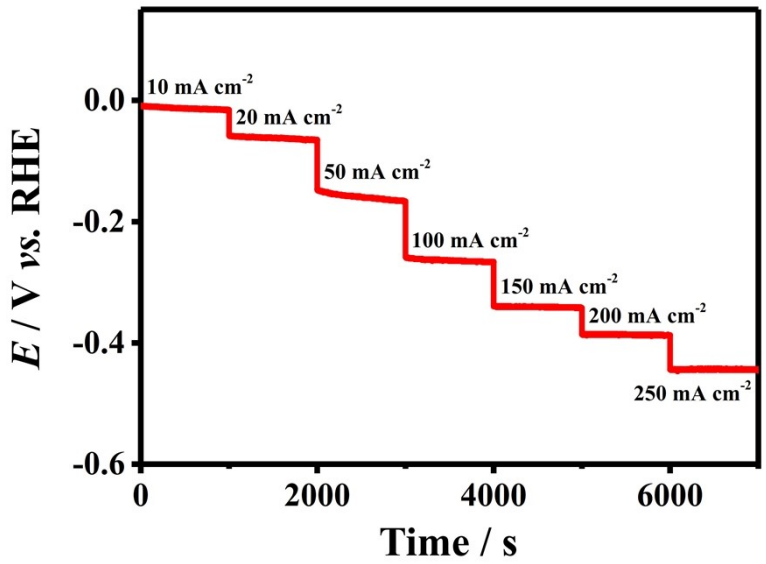

Fig. S11 Multi-current process of the mOsRh/NF. The current density started at 10 mA cm^{-2} and ended at 250 mA cm^{-2} without *iR* correction.

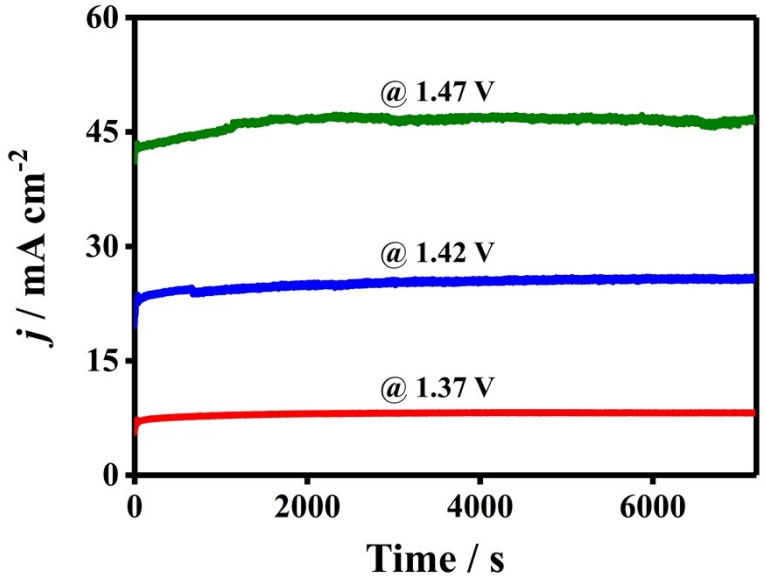

Fig. S12 Chronopotentiometry curves of the mOsRh/NF at different potentials for EOR after 2 h in 1 M KOH with 1 M ethanol.

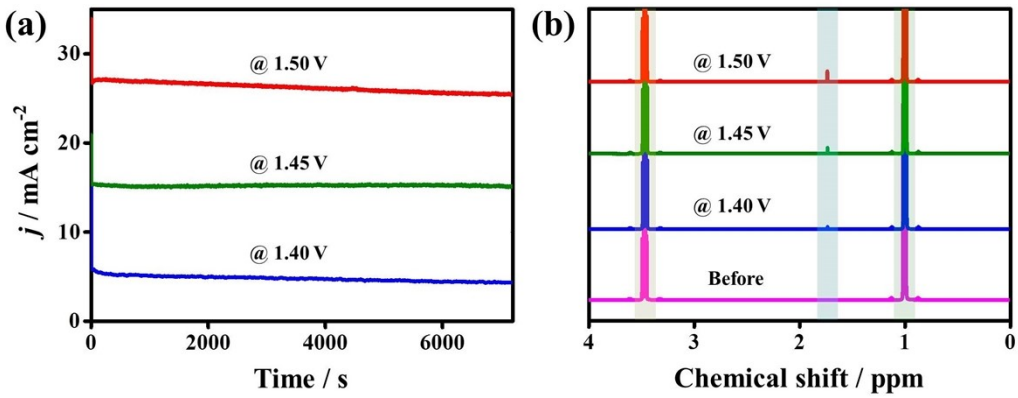

Fig. S13 Chronopotentiometry curves of the mOsRh/NF at different potentials for 2 h in 1 M KOH with 1 M ethanol and the corresponding ^{1}H NMR spectra of electrolytes.

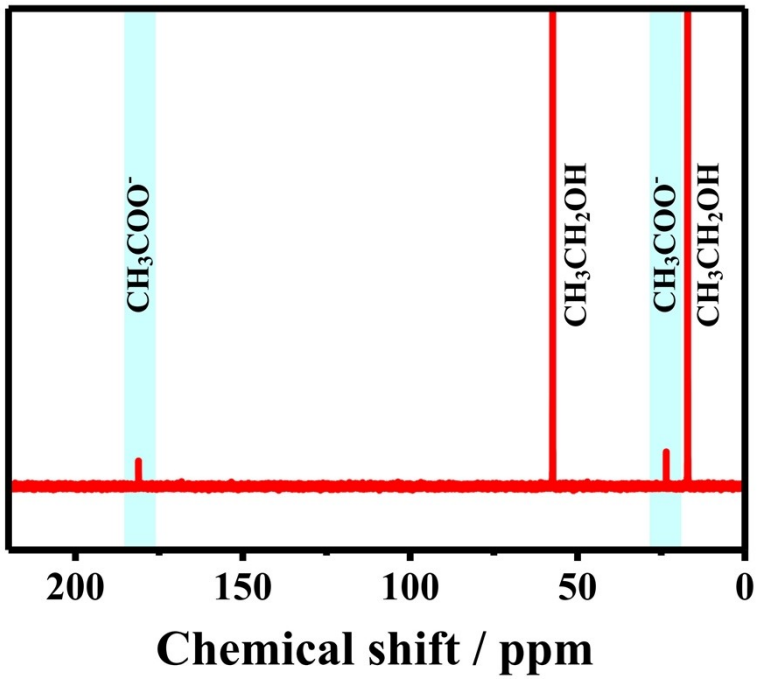

Fig. S14 ^{13}C NMR spectra of electrolyte after long-term stability measurement.

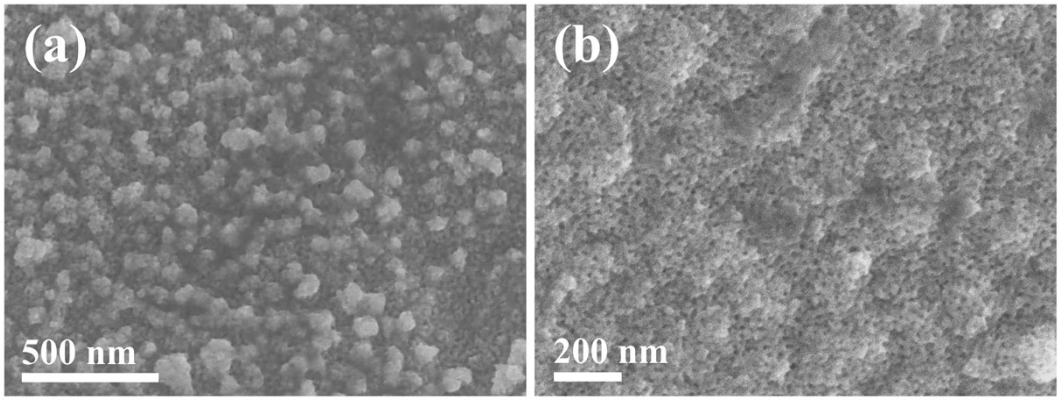

Fig. S15 SEM images of the mOsRh/NF after long-term stability measurement in (a) 1 M KOH for HER and (b) in 1 M KOH+1 M ethanol for EOR.

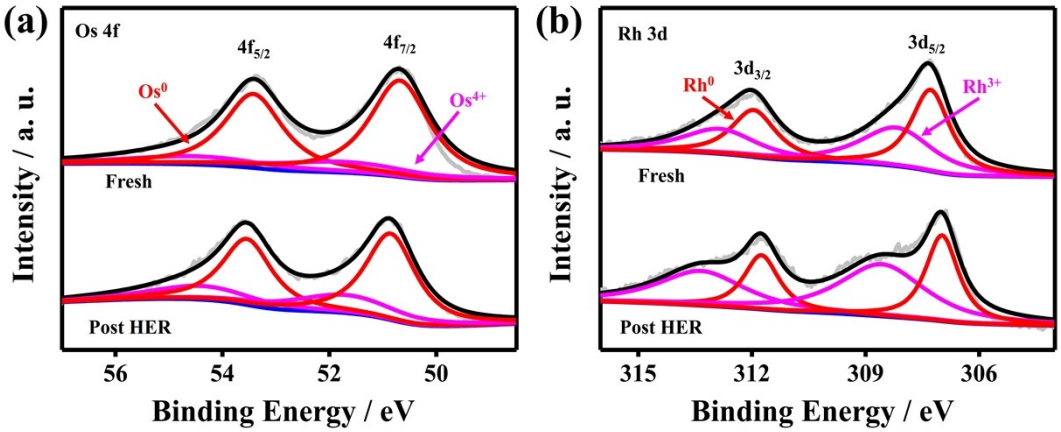

Fig. S16 XPS spectra of the mOsRh/NF after long-term stability measurement for HER.

Table S1 Summary of the representative reports on electrocatalytic HER at ambient conditions.

Catalyst	Electrolyte	Overpotentials	Ref.
mOsRh/NF	**1 M KOH**	**27 mV at 50 mA cm^{-2}** **62 mV at 100 mA cm^{-2}**	**This work**
NF/mRh@PANI	1 M KOH	19 mV at 10 mA cm^{-2} 69 mV at 100 mA cm^{-2}	[1]
$CoNiMoO_4$-21/CuOx/CF	1 M KOH	46 mV at 10 mA cm^{-2} 73 mV at 100 mA cm^{-2}	[2]
Ru–$NiSe_2$/NF	1 M KOH	59 mV at 10 mA cm^{-2} 89 mV at 50 mA cm^{-2}	[3]
F-Ni_3S_4/NF	1 M KOH	29 mV at 10 mA cm^{-2} 92 mV at 100 mA cm^{-2}	[4]
Rh SAC−CuO NAs/CF	1 M KOH	44 mV at 10 mA cm^{-2} 114 mV at 50 mA cm^{-2}	[5]
Ni_2P-Ru_2P/NF	1 M KOH	101 mV at 10 mA cm^{-2} 185 mV at 100 mA cm^{-2}	[6]
pAu_3Pt/NF	1 M KOH	40.1 mV at 50 mA cm^{-2}	[7]
(Ru-Ni)O_x	1 M KOH	14.5 mV at 10 mA cm^{-2} 39.3 mV at 100 mA cm^{-2}	[8]
Pd/$NiFeO_x$ nanosheets	1 M KOH	76 mV at 10 mA cm^{-2} 186 mV at 100 mA cm^{-2}	[9]
NF-Na-Fe-Pt	1 M KOH	31 mV at 10 mA cm^{-2} 96 mV at 50 mA cm^{-2}	[10]

Table S2 Summary of the representative reports of the chemical-assisted hydrogen evolution reaction performance by alcohol of selective oxidation.

Catalyst	Electrolyte	Main anode product	Voltage	Ref.
mOsRh/NF	**1 M KOH + 1 M Ethanol**	**acetic acid**	**1.49 V at 50 mA cm^{-2} 1.53 V at 100 mA cm^{-2}**	**This work**
Co-S-P/CC	1 M KOH + 1 M ethanol	acetic acid	1.63 V at 10 mA cm^{-2}	[11]
NC/Ni-Mo-N/NF	1 M KOH + 0.1 M glycerol	formate	1.38 V at 10 mA cm^{-2}	[12]
Co_3S_4-NSs/Ni-F	1 M KOH + 0.5 M Ethanol	potassium acetate	1.48 V at 10 mA cm^{-2} 1.57 V at 50 mA cm^{-2}	[13]
SA In-Pt NWs	0.5 M ethanol + 1 M KOH	acetate	0.62 V at 10 mA cm^{-2}	[14]
CoNi-PHNs	1 M KOH + 1 M ethanol	acetic acid	1.5 V at 57 mA cm^{-2}	[15]
NiIr-MOF/NF	1 M KOH + 1 M methanol	formate	1.39 V at 10 mA cm^{-2}	[16]
Ni-Fe-P/NF	1 M KOH + 1 M ethanol	acetate	1.53 V at 10 mA cm^{-2}	[17]
F-modified β-FeOOH	1 M KOH + 0.33 M ethanol	acetic acid	1.46 V at 10 mA cm^{-2}	[18]

References

1. Z. Y. Duan, K. Deng, C. J. Li, M. Zhang, Z. Q. Wang, Y. Xu, X. N. Li, L. Wang and H. J. Wang, *Chem. Eng. J.*, 2022, **428**, 132646.

2. M. Gu, X. Deng, M. Lin, H. Wang, A. Gao, X. Huang and X. Zhang, *Adv. Energy Mater.*, 2021, **11**, 2102361.

3. R. Qin, P. Wang, Z. Li, J. Zhu, F. Cao, H. Xu, Q. Ma, J. Zhang, J. Yu and S. Mu, *Small*, 2021, **18**, 2105305.

4. J. Wang, Z. Zhang, H. Song, B. Zhang, J. Liu, X. Shai and L. Miao, *Adv. Funct. Mater.*, 2020, **31**, 2008578.

5. H. Xu, T. Liu, S. Bai, L. Li, Y. Zhu, J. Wang, S. Yang, Y. Li, Q. Shao and X. Huang, *Nano Lett.*, 2020, **20**, 5482-5489.

6. S. Yang, J.-Y. Zhu, X.-N. Chen, M.-J. Huang, S.-H. Cai, J.-Y. Han and J.-S. Li, *Appl. Catal., B.,* 2022, **304**, 120914.

7. H. J. Yu, Z. Q. Wang, Z. C. Dai, Q. Q. Mao, Y. Xu, X. N. Li, L. Wang and H. J. Wang, *Sustainable Energy Fuels*, 2020, **4**, 4878-4883.

8. H. Zhang, Y. Lv, C. Chen, C. Lv, X. Wu, J. Guo and D. Jia, *Appl. Catal., B.,* 2021, **298**, 120611.

9. W. Zhang, X. Jiang, Z. Dong, J. Wang, N. Zhang, J. Liu, G. R. Xu and L. Wang, *Adv. Funct. Mater.*, 2021, **31**, 2107181.

10. Y. Zhao, Y. X. Gao, Z. Chen, Z. J. Li, T. Y. Ma, Z. X. Wu and L. Wang, *Appl. Catal., B.,* 2021, **297**., 120395.

11. S. Sheng, K. Ye, L. N. Sha, K. Zhu, Y. Y. Gao, J. Yan, G. L. Wang and D. X. Cao, *Inorg. Chem. Front.*, 2020, **7**, 4498-4506.

12. Y. Xu, M. Y. Liu, S. Q. Wang, K. L. Ren, M. ZWang, Z. Q. Wang, X. N. Li, L. Wang and H. J.

Wang, *Appl. Catal., B.,* 2021, **298**, 120493.

13. Y. Ding, Q. Xue, Q. L. Hong, F. M. Li, Y. C. Jiang, S. N. Li and Y. Chen, *ACS Appl. Mater. Interfaces*, 2021, **13**, 4026-4033.

14. Y. Zhu, X. Zhu, L. Bu, Q. Shao, Y. Li, Z. Hu, C. T. Chen, C. W. Pao, S. Yang and X. Huang, *Adv. Funct. Mater.*, 2020, **30**, 2004310.

15. W. Wang, Y. B. Zhu, Q. Wen, Y. Wang, J. Xia, C. Li, M. W. Chen, Y. Liu, H. Li, H. A. Wu and T. Zhai, *Adv. Mater.*, 2019, **31**, 1900528.

16. Y. Xu, M. Y. Liu, M. Z. Wang, T. L. Ren, K. L. Ren, Z. Q. Wang, X. N. Li, L. Wang and H. J. Wang, *Appl. Catal., B,* 2022, **300,** 120753.

17. S. Sheng, Y. P. Song, L. N. Sha, K. Ye, K. Zhu, Y. Y. Gao, J. Yan, G. L. Wang and D. X. Cao, *Appl. Surf. Sci.*, 2021, **561**, 150080.

18. G.-F. Chen, Y. Luo, L.-X. Ding and H. Wang, *ACS Catal.*, 2017, **8**, 526-530.